Available online at www.sciencedirect.com
ScienceDirect
Journal of Nuclear Materials 374 (2008) 204–210
journal of nuclear materials
www.elsevier.com/locate/jnucmat

Evaluation of pre-transition oxide on Zr–0.4 Nb alloy by using the HVEM

Hyun-Gil Kim *, Jeong-Yong Park, Byung-Kwon Choi, Yong-Hwan Jeong

Advanced Core Materials Lab, Korea Atomic Energy Research Institute, 150 Doekjin-dong, Yuseong-gu, Daejeon 305-353, Republic of Korea

Received 30 March 2006; accepted 3 August 2007

Abstract

The crystalline structure and morphology of zirconium oxide formed in a water at 360 °C and 18.9 MPa was investigated by using a high voltage electron microscopy (HVEM). The oxide thickness formed on the Zr–0.4 Nb alloy substrate was about 2.2 μm. In the thin oxide layer, the monoclinic and tetragonal phases were mixed with each other and a complex morphology of equiaxed and columnar grains were formed during the oxidation process. From the HVEM observation and the imaging process by using the DigitalMicrograph™ program, it was found that the correlation of a crystalline orientation between the equiaxed grain and the columnar grain was not formed in the oxide layer, and a defect such as a dislocation which had formed in the tetragonal phase could be extracted by the masking tool of the inverse fast Fourier transformation (IFFT).

1. Introduction

The Zr-based alloys used as fuel cladding in a nuclear reactor have good corrosion resistance and mechanical properties at a high temperature and neutron stability. Corrosion behavior of the zirconium alloys is controlled by the properties of oxide which is formed during high temperature oxidation [1–3]. It is well known that the formation of an oxide layer is caused by oxygen ion diffusion into a zirconium substrate at high temperature and these oxide properties are generally divided by two significant characteristics such as the crystalline structure of the tetragonal and monoclinic phases and the morphology of columnar and equiaxed grain shapes. From the results of researches on oxide properties, the existence of a tetragonal zirconia phase and a columnar grain structure in an oxide has been shown to be the main reason for the good corrosion behavior of Zr-based alloys [4–7]. However, some researchers found that the volume fraction of the tetragonal phase was not directly matched with the corrosion resistance, from a micro-beam X-ray diffraction analysis for the oxides formed on Zr-based alloys (Zircaloy-4 and high Nb-containing Zr alloys) [8]. It was thought that the different results for the correlation between the tetragonal phase volume fraction and the corrosion rate may be related to the calculation method of the tetragonal phase volume fraction, because most of the results did not consider a texture correction of the oxides besides the results of Yilmazbayhan and Motta. Also, it was caused by the resolution of the applied techniques such as a bulk X-ray diffraction and Raman spectroscopy when compared to a micro-beam synchrotron radiation.

From the results of a zirconium oxide characterization, the tetragonal oxide phase is stabilized by high compressive stresses at a metal/oxide interface [4]. Especially, the stabilization of a tetragonal phase with an applied pressure was measured by using Raman spectroscopic studies [9]. According to their observation, the monoclinic ZrO_2 phase transforms to the tetragonal phase at about 3.5 GPa. Also, Garvie reported that tetragonal zirconia at room temperature appeared in active powders of ZrO_2 characterized by a small mean crystal size, a large specific energy and an appreciable excess energy [10]. Tomaszewski and Godwod

* Corresponding author. Tel.: +82 42 868 2522; fax: +82 42 862 0432.
E-mail address: hgkim@kaeri.re.kr (H.-G. Kim).

0022-3115/$ - see front matter © 2007 Elsevier B.V. All rights reserved.
doi:10.1016/j.jnucmat.2007.08.003

investigated the critical values of an oxygen vacancy concentration reasonable for the meta-stability of zirconia and they estimated that the critical value of the oxygen vacancy concentration for a tetragonal form is 3% [11]. Therefore, a meta-stable tetragonal zirconia phase at room temperature can be stabilized by the effects such as a compressive stress, a small size grain, and a low stoichiometry.

Recently, to study the oxide characteristics of zirconium alloy, many techniques such as a synchrotron X-ray diffraction [8,12] and high resolution transmission electron microscopy (HRTEM) [7,13] have been introduced to analyze oxide layers. In the micro X-ray diffraction experiment by using a synchrotron, a periodic intensity variation of the tetragonal phase fraction was observed in an oxide layer [8]. From the view point of an oxide crystal structure, it was reported that the volume fraction of a tetragonal zirconia structure was increased near a metal/oxide interface more so than that in the outer parts of oxide layers [8], and a substoichiometric zirconium oxide layer was observed in pre-transition oxides [13].

In this study, the microstructure of oxides formed on Zr–0.4 Nb alloy was characterized by using a high voltage electron microscopy of 1250 keV. The high resolution image analysis used in this study can provide more detailed information on a zirconium oxide which is not available in previous results.

2. Experimental procedure

The sample for the oxide analysis of zirconium alloy was selected on the binary alloy of Zr–0.4 wt% Nb. The alloy was prepared by the vacuum arc remelting method with sponge zirconium and high purity (99.99%) niobium and then this ingot was beta-solution treated at 1050 °C for 30 min. The quenched ingot was hot-rolled after pre-heating at 580 °C for 10 min and cold-rolled three times to a final thickness of 0.8 mm. Between the rolling steps, the cold-rolled sheet was intermediate-annealed at 580 °C. Specimens for the corrosion test, 25 by 20 by 0.8 mm in size, were cut from the manufactured strip, mechanically ground up to 1200 grit SiC paper, and then pickled in a solution of 5 vol.% HF, 45 vol.% HNO_3 and 50 vol.% H_2O. The corrosion test was performed in a static autoclave with distilled water under the condition of 360 °C and 18.9 MPa according to the procedure of ASTM G2-88. Therefore, the sample for the oxide characterization was obtained from the Zr–0.4 Nb alloy which was corroded for 90 days. For the TEM observation of the oxide, the sections with oxide in the corroded samples were glued to each other and they were inserted into stainless steel tube, and then they were sliced into a thickness of about 300 μm from the perpendicular direction to the oxide/metal interface. The sliced specimens were mechanically polished until their thickness became about 20 μm and then they were finally given an ion-milling.

In this study, two different transmission electron microscopes were used to characterize the cross sectional oxide layer formed on the Zr–0.4 Nb alloy. One is a 200 keV JEOL 2010 conventional transmission electron microscope, where the point resolution is 0.31 nm, at Korea Atomic Energy Research Institute (KAERI). The other is a 1250 keV JEOL high voltage electron microscope, where the point resolution of this microscopy is 0.117 nm, at Korea Basic Science Institute (KBSI). The HVEM had a good point resolution and also a large penetration depth for the specimens more so than the conventional TEM. So it is possible that high quality resolution images could be obtained from the HVEM observation in the case of a specimen with a thick thickness. The diffraction information was contained in the HVEM images. Therefore, the observed images from the HVEM could be analyzed by the Fourier mask filtering method which was performed by using the DigitalMicrograph™ (DM, Gatan Inc.) program. The Fourier mask filtering method is one of the techniques to enable a quantitative analysis of experimentally high resolution TEM images [14,15].

3. Results and discussion

Generally, the microstructure of a zirconium oxide formed at a reactor operating temperature is known to consist of equiaxed and columnar shape grain morphologies. Fig. 1 shows the overall microstructure of the cross sectional oxide on the Zr–0.4 Nb alloy from an oxide/metal interface to the outer part of the oxide formed on the Zr–0.4 Nb alloy. This microstructural image was obtained by conventional transmission electron microscopy. The oxide thickness was about 2.2 μm and the oxide microstructure could be divided into three regions as shown in Fig. 1. The oxide consists of an equiaxed grain structure in the outer oxide surface, a columnar grain structure in

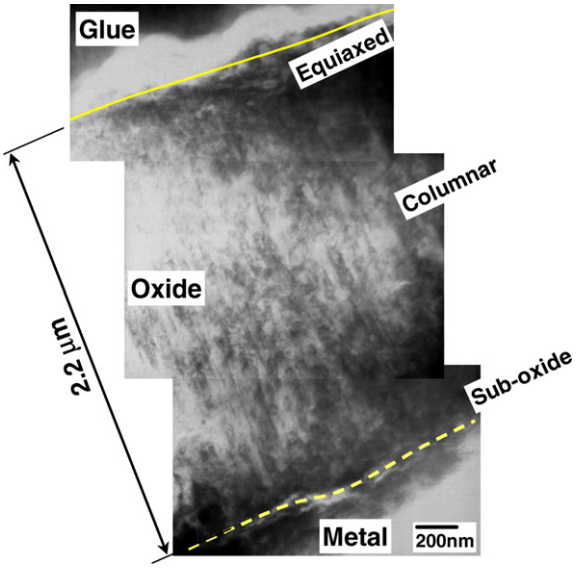

Fig. 1. Cross-sectional TEM micrographs of the zirconium oxide formed on Zr–0.4 Nb alloy at 360 °C, water.

the middle area, and an irregular structure at the oxide/metal interface.

The general features of the oxide formation could be observed from Fig. 1. Small equiaxed oxide grains were formed at the initial stage of corrosion, and columnar grains were grown from some equiaxed grains to minimize the compressive stress, and an oxide/metal interface region which was a new layer for a nucleation site, was formed at an oxide/metal interface. This was in good agreement with previous results for the microstructural characteristics with the oxide thickness and the location of the zirconium oxide layer [6,13,16]. However, more detailed information on the oxide microstructure at the equiaxed/columnar grain boundaries and in the oxide/metal interface is somewhat insufficient. Therefore, a microstructural observation was performed using a high voltage electron microscopy with a good point resolution of 0.117 nm.

Fig. 2 shows the high voltage electron microscope image, which was obtained from the boundary between the equiaxed and columnar grain in the outer oxide region. Although the grain boundaries were not clearly seen in this figure, the small equiaxed grains and a portion of the columnar grains were identified in the image.

In Fig 2, some lattice images of the equiaxed and columnar grains were unclear. It is thought that the unclear lattice images are caused by a large difference of zone axis among the grains in the oxide layer, because these lattice images could be more clearly seen from a sample tilting. So it is assumed that the observation of an unclear grain image is related to a high order misorientation of the oxide grains.

The oxide grains in the picture were revealed as a tetragonal ZrO_2 phase and a monoclinic ZrO_2 phase from the lattice image analysis by using the DIFPACK tools contained in the DigitalMicrograph™ program. The observation of unidentified grains was related to the high angle of the crystalline orientation between the grains. It was observed that the (0 1 1) monoclinic plane of the columnar grain had an angle of 38° with respect to the (0 0 2) tetragonal plane of the equiaxed grain, and designated as A and A′, and the angle between the (1 1 0) monoclinic plane of the columnar grain and the (1 0 1) tetragonal plane of the equiaxed grain was determined as 34° and designated as B and B′. From this result, although it was observed that the monoclinic phases marked as Á and Ḃ were formed near the tetragonal phases designated as A and B, it was difficult to find the any crystal orientation relationship between the monoclinic phase with a columnar shape and the tetragonal phase with an equiaxed shape in this work.

Fig. 3 shows the columnar oxide grains observed at the middle region of the zirconium oxide. The upper right region in the image was darker than the other regions. It was caused by a difference of the sample thickness, because a uniform sample thickness could not be obtained from the ion-milling process. Since it should be assumed that a lattice array is almost similar for the same grain of a columnar shape, the analysis was performed for a clear region in the image. The (1 1 1) monoclinic plane of the columnar grain was aligned at about 45° from the oxide growth direction, designated as A and the (0 2 0) monoclinic plane of the columnar grain was aligned at about 70° from the oxide growth direction, designated as B. In the literature, it was reported that the growth direction of the columnar grains was apparently oriented to have a specific orientation. The (1 1 1) monoclinic poles are orientated at about 40–70° away from the oxide surface normal and the (2 0 0)

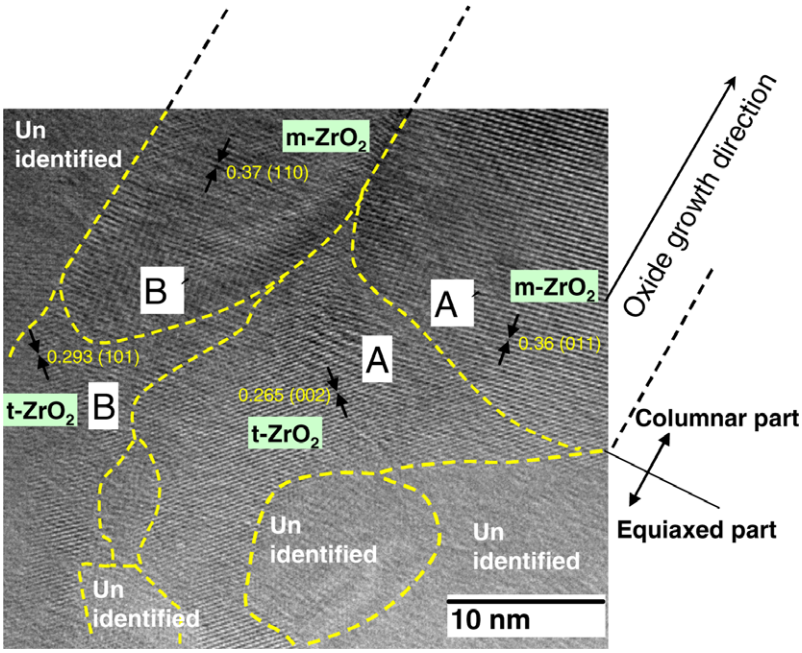

Fig. 2. HVEM image for the equiaxed and columnar grains in the outer oxide layer.

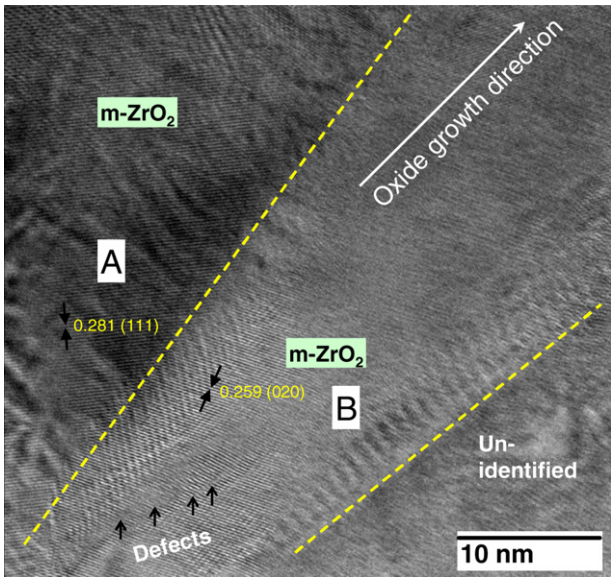

Fig. 3. HVEM image for the columnar grain area in the middle oxide layer.

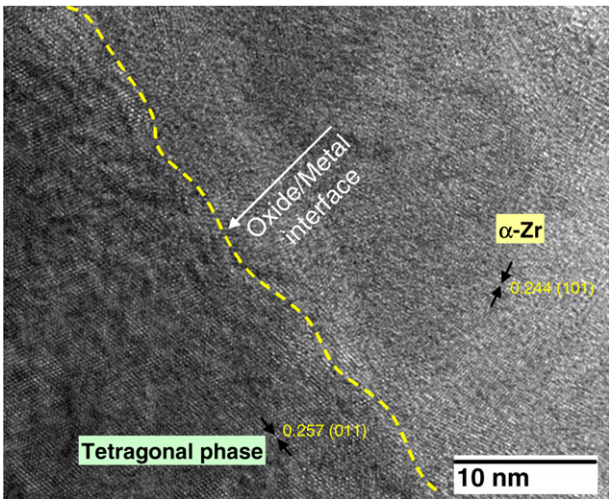

Fig. 4. HVEM image for the oxide/metal interface area in the inner oxide layer.

monoclinic poles which are orientated nearly parallel to the oxide growth direction [16]. The (1 1 1) monoclinic plane observed in this study was matched well with a previous result [16]. However, a crystalline orientation of the (0 2 0) monoclinic plane to the oxide growth direction has not been reported.

In Fig. 3, a defect could not be found in the (1 1 1) monoclinic plane of the columnar grain whereas many defects were found in the (0 2 0) monoclinic plane of the columnar grain, designated as arrows. Since the (0 2 0) monoclinic plane was more parallel to the sample surface than the (1 1 1) plain, it was assumed that the compressive stress of the (0 2 0) plane was accumulated more in the perpendicular direction when compared to the (1 1 1) plane. So it is thought that the amount of defects will be increased in the case of a more perpendicular direction to the compressive stress in the columnar oxide plane. Also the (0 2 0) monoclinic plane disappeared at the middle area in the columnar grain. The texture evaluation of the oxide was limited by using the high resolution lattice image because the observed area of the oxide was very small.

Wadman et al. observed a few columnar tetragonal grains and equiaxed monoclinic grains in the outer part of the oxide layer in a standard Zircaloy-4 and they did not mention observing the columnar tetragonal grains in the oxide formed on the Zr–0.5 Sn–0.53 Nb alloy [17]. The columnar tetragonal grains were not detected in this study. So the formation of the columnar tetragonal grains was related to the alloying composition between Zircaloy-4 and Zr–0.4 Nb alloy.

Fig. 4 shows the high resolution image observed at an oxide/metal interface. The characteristics of an oxide/metal interface are very important because a corrosion behavior is determined by the oxide/metal interface characteristics. From the high resolution image of the oxide/metal interface, a large grain with a grain size of about 100 nm was observed in the oxide side and a wavy interface between the metal and oxide was formed. The wavy interface was formed between the large grain and the α-Zr grain. The approximate width and height in the waves was about 8 nm and 2 nm, respectively. Since this wavy interface was very small at a nm scale between the grains, it was spontaneously formed by an oxygen diffusion from the oxide part to the metal part during the oxidation process.

Structure of the metal/oxide interface is not well defined. However, the existence of a sub-oxide grain or layer has already been reported [13,16]. Anada and Takeda [13] observed two layers in a pre-transition oxide such as 50–80 nm thick layers of tetragonal ZrO_2 grains near an oxide/metal interface and a 200 nm thick substoichiometric oxide layer containing 'distorted' monoclinic ZrO_2 and α-Zr, and also containing 10 nm equiaxed oxide grains. These layers were seen in pre-transition oxides of Zircaloy-4, Zircaloy-2 and Zircaloy-4 with a 1% Nb added alloy. These layers were not seen in the post-transition oxide of Zircaloy-4. Yilmazbayhan et al. [16] reported that an oxide/metal interface region, named a blocky grain, contained small tetragonal particles. In this study for the Zr–0.4 Nb alloy in the pre-transition oxide, the oxide–metal interface region observed in this study consisted of a large sized tetragonal phase as shown in Fig. 5. In this region of a high resolution image, some contrasts with 2–3 nm in a globular shape were observed. Also, an un-identified area of a few nm in width existed between the tetragonal phase and the α-zirconium shown in Fig. 5. From this result, tetragonal oxide was not directly formed on the zirconium matrix.

To analyze the contrast region in more detail, the techniques of an image quality enhancement by the fast Fourier transform (FFT) and Fourier mask filtering techniques were applied for the atomic resolution image. The data processes of the FFT and Fourier mask filtering are summarized in Fig. 6. Each image process for the data was per-

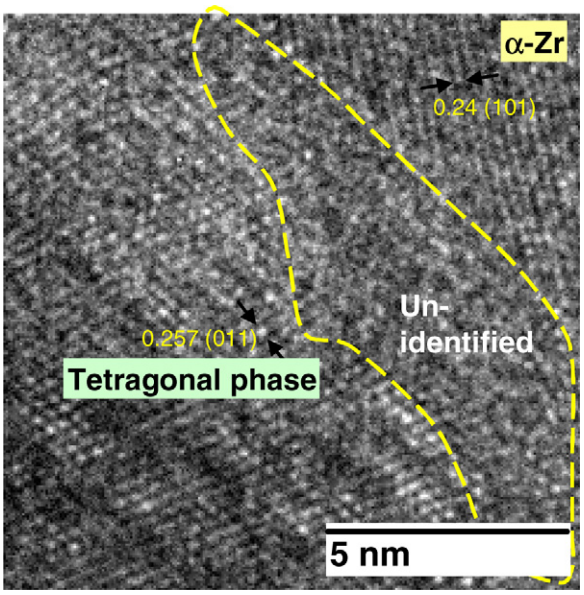

Fig. 5. Atomic lattice image for the oxide/metal interface.

formed by using the DigitalMicrograph™ (DM, Gatan Inc.) program. A good agreement was found between the HVEM observation image (a) and the IFFT image (e). Because the inverse FFT (IFFT) image was clearer than the original image, it was possible to extract a defect by the mask filtered pattern from the IFFT operation image.

Fig. 7 shows the mask filtered pattern and IFFT results of the tetragonal phase. All the planes of the tetragonal phase are shown in Fig. 7(a) and each plane of the tetragonal phase is shown in Fig. 7(b). In Fig. 7(b), the transformed lattice image in the right hand side was obtained from the mask filtered pattern image of each tetragonal phase plane in the left hand side. The transformed images

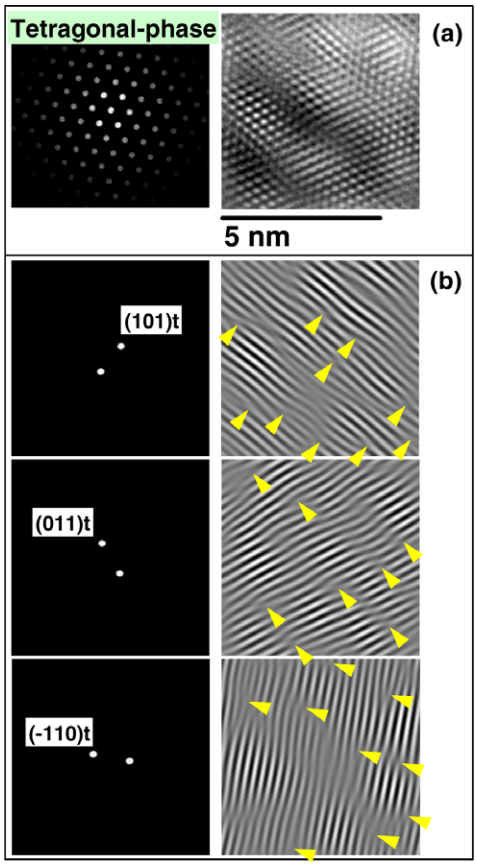

Fig. 7. Reconstruction of the phase contrast image of the tetragonal phase observed in the oxide/metal interface region.

indicate that many defects, marked as arrows, were observed in the tetragonal phase of a large grain. It could be concluded that the dislocations were formed by an oxygen vacancy because the stoichiometry of the zirconium

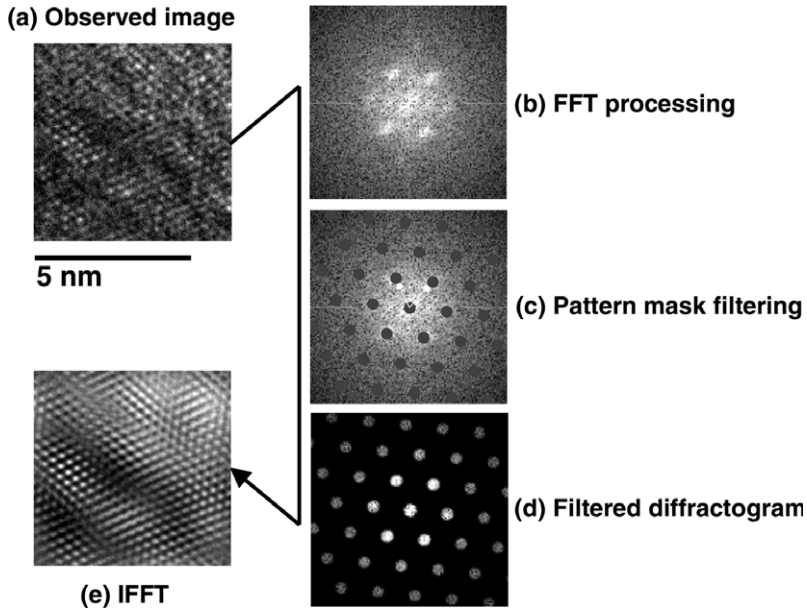

Fig. 6. Image processing method using the fast Fourier transform (FFT) and Fourier mask filtering techniques.

oxide (ZrO_2) was not satisfied in the oxide/metal interface region.

In the oxides formed on the zirconium alloys, a mechanism for stabilizing the tetragonal phase has been reported [18–20]. The tetragonal phase is stabilized by high stresses in the oxides near an oxide/metal interface [18] and it is also stabilized when the grain size is smaller than 30 nm [19]. It is also known that lower valence state elements (Y, Ca, etc.) in zirconia could help to stabilize the tetragonal phase. The oxygen vacancies were associated with the tetragonal and cubic phases [20]. It was assumed that the tetragonal phase observed in the outer oxide region was stabilized by the effects of a small grain size, since the observed grain size of the tetragonal phase was smaller than 30 nm in diameter. However, since a tetragonal phase with a large grain size up to 100 nm in diameter was observed in the metal/oxide interface, it is believed that a large size of the tetragonal phase was stabilized by the effects of high stresses and oxygen vacancies. To confirm the stress between the small size tetragonal phase in the outer region and the large size tetragonal phase in the metal/oxide interface region, a *d*-spacing of the tetragonal phases was considered. Since the observed tetragonal phase grains were random in the oxide, the direction of the analyzed *d*-spacing planes was difference in the oxide layer. In the outer region, the most frequently observed plane of the equiaxed tetragonal phase was (0 0 2) and the most frequently observed plane of the large size tetragonal phase was (0 1 1) in the metal/oxide region. Therefore, a comparison of the *d*-spacing was performed for the (0 0 2) plane, which was most frequently observed in the outer oxide region, and for the (0 1 1) plane, which was most frequently observed in the metal/oxide interface region. The *d*-spacing, which was obtained from the HVEM image, was compared to the JCPDS (42-1164; zirconium oxide). Since the distance of the (0 0 2) tetragonal phase plane in the outer oxide region was 0.265 nm and that of the (0 1 1) tetragonal phase plane in the metal/oxide region was 0.257, it was shown that the *d*-spacing of the (0 0 2) tetragonal phase was increased from 0.2635 nm to 0.265 nm and that of the (0 1 1) tetragonal phase was decreased from 0.2574 nm to 0.257 nm when compared to the JCPDS, respectively. From this result, it was shown that the stress of the (0 0 2) tetragonal phase in the outer oxide region was released more and that of the (0 1 1) tetragonal phase in the metal/oxide interface region was accumulated more. So, it is assumed that the applied stress in the tetragonal phases was higher in the metal/oxide region than in the outer oxide region. Godlewski et al. mentioned that a stress relaxation due to the dissolution of a metal has caused a tetragonal phase to transform to a monoclinic phase, accompanied by the crack formation [18]. In the present study, the reason for the observation of the tetragonal phase in the oxide layer is assumed to be that the zirconium matrix remained and cracks were not formed in the whole oxide layer after the sample preparation steps. The existence of many defects in the tetragonal phase was caused a decrease of the *d*-spacing of large scale tetragonal phase in the metal/oxide region.

From this result, the stability mechanism of the tetragonal phase in the oxide layer was different depending on the oxide thickness. In this study, the information of the oxide layer by using a high resolution TEM image was limited because the HVEM observation of the oxide layer was very difficult to observe for the whole oxide area. However, information on the equiaxed and columnar grain boundaries, columnar grain structure, and the oxide/metal interface region for the oxide formed on the Zr–0.4 Nb alloy was obtained from this study. To obtain more detailed information for all the cross-sectional directions of the oxide layer, additional work is required.

4. Conclusion

In the present study, the oxide characteristics of a pretransition oxide formed on Zr–0.4 Nb alloy were investigated by using the HVEM.

From the observations for the equiaxed and columnar grain interfaces, although the monoclinic phase was grown from a tetragonal phase, a crystalline orientation relationship between the monoclinic phase of a columnar shape and the tetragonal phase of an equiaxed shape was not found.

From the high resolution image of the oxide/metal interface, a tetragonal phase of a large grain with a grain size of about 100 nm was observed in the oxide. The tetragonal oxide was not directly formed on the zirconium matrix. And the transformed images by using the IFFT image process indicated that many defects were formed in the tetragonal phase of a large grain.

Acknowledgements

This study was supported by Korean Government, through its national nuclear technology program. The authors would like to thank KBSI for High Voltage Electron Microscopy (HVEM).

References

[1] J.A. Whitton, J. Electronchem. Soc. 115 (1968) 58.
[2] B. CoxAdvanced in Corrosion Science and Technology, vol. V, Plenum, New York, 1976, p. 173.
[3] B. Cox, AECL-3285, Atomic Energy of Canada Ltd., Chalk River Nuclear Lab., 1965.
[4] F. Garzarolli, H. Seidel, R. Tricot, J.P. Gros, ASTM STP 1132 (1991) 395.
[5] P. Bouvier, J. Godlewski, G. Lucazeau, J. Nucl. Mater. 300 (2002) 118.
[6] Y.H. Jeong, H.G. Kim, T.H. Kim, J. Nucl. Mater. 317 (2003) 1.
[7] H.G. Kim, Y.H. Jeong, T.H. Kim, J. Nucl. Mater. 326 (2004) 125.
[8] A. Yilmazbayhan, A.T. Motta, R.J. Comstock, G.P. Sabol, B. Lai, Z. Cai, J. Nucl. Mater. 324 (2004) 6.
[9] H. Arashi, M. Ishigame, Phys. Stat. Sol. (a) 71 (1982) 313.
[10] R.C. Garvie, J. Phys. Chem. 64 (4) (1965) 1238.

[11] H. Tomaszewski, K. Godwod, J. Euro. Ceram. Soc. 15 (1995) 17.
[12] J.Y. Park, H.G. Kim, Y. H Jeong, Y.H. Jung, J. Nucl. Mater. 335 (2004) 433.
[13] H. Anada, K. Takeda, ASTM STP 1295 (1996) 35.
[14] Z.-Q. Liu, M. Song, K. Mitsuishi, H. Hashimoto, J. Electron. Microsc. 53 (2) (2004) 146.
[15] M. Rowicka, A. Kudlicki, Z. Otwinowski, Acta Cryst. A 58 (2002) 574.
[16] A. Yilmazbayhan, E. Breval, A.T. Motta, R.J. Comstock, J. Nucl. Mater. 439 (2006) 265.
[17] B. Wadman, Z. Lai, H.-O. Andren, A.-L. Nystrom, P. Rudling, H. Pettersson, ASTM STP 1245 (1994) 579.
[18] J. Godlewski, J.P. Gros, M. Lambertin, J.F. Wadier, H. Weidinger, ASTM STP 1132 (1991) 416.
[19] P. Barberis, J. Nucl. Mater. 226 (1995) 34.
[20] S. Fabris, A.T. Paxton, M.W. Finnis, Acta Mater. 50 (2002) 5171.